

pubs.acs.org/joc Article

# Gas Phase Experimental and Computational Studies of AlkB Substrates: Intrinsic Properties and Biological Implications

Lanxin Zhang, Xiao Ding, Catherine R. Kratka, Alec Levine, and Jeehiun K. Lee\*



Cite This: J. Org. Chem. 2023, 88, 13115–13124



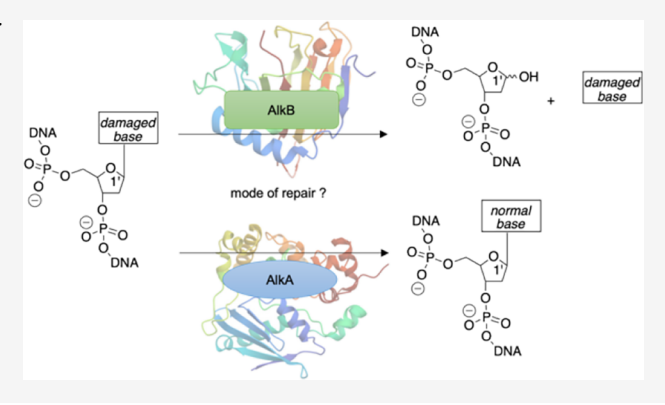
**ACCESS** I

III Metrics & More

Article Recommendations

Supporting Information

**ABSTRACT:** The gas phase acidity and proton affinity of nucleobases that are substrates for the DNA repair enzyme AlkB have been examined using both computational and experimental methods. These thermochemical values have not heretofore been measured and provide experimental data that help benchmark the theoretical results. We also use our gas phase results to lend insight into the AlkB mechanism, particularly in terms of the role AlkB plays in DNA repair, versus its complementary enzyme AlkA.



# **■ INTRODUCTION**

The maintenance of DNA integrity is essential for all living organisms. Unfortunately, DNA is constantly under assault, from both cellular metabolites and exogenous agents. Such damage compromises cell function, causes incorrect propagation of the genetic code, and is associated with carcinogenesis. 1,2

The genome is preserved with the support of DNA repair pathways. <sup>1–5</sup> In *Escherichia coli*, exposure to DNA-methylating agents leads to upregulation of a series of enzymes, in what is called "the adaptive response". <sup>3,6</sup> Two prominent enzymes in this response are AlkA and AlkB (Figure 1). AlkA participates in the base excision repair (BER) pathway; it is a glycosylase that cleaves the damaged base by breaking the *N*-glycosidic bond heterolytically (Figure 1). <sup>1,2</sup> AlkB follows an alternate path, by directly reversing the base damage chemically, to yield the repaired, normal base (Figure 1). <sup>7–15</sup>

Both AlkA and AlkB are particularly intriguing, as both enzymes accept a wide range of substrates. Herein, we examine the gas phase acidity and proton affinity of a series of AlkB substrates. In our prior work, we have found that the examination of properties in the gas phase, which provides the "ultimate" nonpolar environment, uncovers intrinsic, inherent reactivity that correlates with activity in other nonpolar media, including hydrophobic enzyme active sites. <sup>16–19</sup> We discuss our results in the context of the differing mechanisms by which AlkA and AlkB process lesions.

# RESULTS

**1-Methyladenine (1meA, 1).** *Calculations: Tautomers, Acidity, Proton Affinity, 1meA.* In our experience, density

functional theory (DFT) methods generally yield accurate values for thermochemical properties of nucleobases. 
Therefore, we utilized B3LYP-D3(BJ)/6-311++G(2d,p) to calculate the relative tautomeric stabilities (relative enthalpies), acidities ( $\Delta H_{\rm acid}$ ), and proton affinities (PA) of 1-methyladenine (1, 1meA). This method includes a large basis set and, importantly, accounts for dispersion. Various tautomers can be drawn for 1meA; those within 10 kcal/mol of the most stable tautomer are shown in Figure 2 (remaining tautomers are in the Supporting Information (SI)). The most stable tautomer (imine N9-H structure 1a) is calculated to be 3.8 kcal/mol more stable than its N7-H counterpart (structures 1b and 1c). The most acidic site of 1a is predicted to be N9-H ( $\Delta H_{\rm acid}$  = 337.4 kcal/mol). The most basic site of tautomer 1a is the exocyclic N6 (PA = 241.6 kcal/mol).

Experiments: Acidity, 1meA. We previously bracketed the acidity of 1meA to be roughly  $334 \pm 3 \text{ kcal/mol.}^{21,22}$ 

Experiments: Proton Affinity, 1meA. We measured the proton affinity of 1meA using PA bracketing (Table 1; see the Experimental Section for additional details). The reaction with tributylamine (PA =  $238.6 \pm 2$  kcal/mol) occurs in both directions; meaning, 1meA can deprotonate protonated tributylamine and tributylamine can deprotonate protonated 1meA. We therefore bracket the PA to be  $239 \pm 3$  kcal/mol.

Received: June 15, 2023 Published: August 31, 2023





Figure 1. The different paths by which AlkA and AlkB process DNA lesions.

Figure 2. Calculated data for 1-methyladenine. Gas phase acidities are in red; gas phase proton affinities are in blue. Relative stabilities are in parentheses. Calculations were conducted at B3LYP-D3(BJ)/6-311++G(2d,p); reported values are  $\Delta H$  at 298 K, in kcal/mol.

Table 1. PA Bracketing of 1meA (1)

		proton transfer <sup>b</sup>	
reference base	PA (kcal/ mol) <sup>a</sup>	ref base	conj acid
1-pyrrolidino-1-cyclopentene	$243.6 \pm 2.0$	+	_
N,N,N',N' - tetramethylethylenediamine	$242.1 \pm 2.0$	+	_
tributylamine	$238.6 \pm 2.0$	+	+
N,N-dimethylcyclohexylamine	$235.1 \pm 2.0$	_	+
2,4-lutidine	$230.1 \pm 2.0$	_	+
4-picoline	$226.4 \pm 2.0$	_	+

<sup>a</sup>Ref 23 <sup>b</sup>A "+" indicates the occurrence and "–" indicates the absence of proton transfer.

The proton affinity of 1meA was also measured by the Cooks kinetic method. High Paragraph 248.2  $\pm$  2.0 kcal/mol), N,N,N',N'-tetramethyl-1,8-napthalene (PA = 245.8  $\pm$  2.0 kcal/mol), N,N'-dimethyl-1,3-propanediamine (PA = 245.0  $\pm$  2.0 kcal/mol), 1-pyrrolidino-1-cyclopentene (PA = 243.6  $\pm$  2.0 kcal/mol), N,N,N',N'-tetramethylethylenediamine (PA = 242.1  $\pm$  2.0 kcal/mol), N,N-diisopropylethylamine (PA = 237.6  $\pm$  2.0 kcal/mol), N,N'-dimethylethylenediamine (PA = 236.4  $\pm$  2.0 kcal/mol)

kcal/mol), and *N,N*-dimethylcyclohexylamine (PA =  $235.1 \pm 2.0 \text{ kcal/mol}$ ), yielding a PA for 1meA of  $244 \pm 3 \text{ kcal/mol}$ .

1-Methylguanine (1meG, 2). Calculations: Tautomers, Acidity, Proton Affinity, 1meG. 1-Methylguanine (1meG, 2) has four tautomers within 10 kcal/mol of the most stable tautomer (Figure 3). The most acidic site of 2a is the N7 site, at 340.3 kcal/mol. The most basic site of 2a is the N9, with a PA of 232.3 kcal/mol. Tautomer 2b is just 0.9 kcal/mol less stable than 2a. The acidity of 2b is 339.4 kcal/mol, at the N9-H site, and the PA is 233.2 kcal/mol, at the N7 site.

Experiments: Acidity, 1meG. 1-Methylguanine is an involatile solid, and we were unable to conduct bracketing experiments. However, we were able to use the Cooks kinetic method to ascertain thermochemical properties. The acidity of 1-methylguanine was measured using nine reference acids: methoxyacetic acid ( $\Delta H_{\rm acid} = 341.9 \pm 2.1 \, \rm kcal/mol$ ), phenylacetic acid ( $\Delta H_{\rm acid} = 341.5 \pm 2.1 \, \rm kcal/mol$ ), benzoic acid ( $\Delta H_{\rm acid} = 340.1 \pm 2.2 \, \rm kcal/mol$ ), 2-fluorobenzoic acid ( $\Delta H_{\rm acid} = 338.0 \pm 2.2 \, \rm kcal/mol$ ), anthranilic acid ( $\Delta H_{\rm acid} = 337.3 \pm 2.2 \, \rm kcal/mol$ ), 3-fluorobenzoic acid ( $\Delta H_{\rm acid} = 335.9 \pm 2.1 \, \rm kcal/mol$ ), 4-hydroxybenzoic acid ( $\Delta H_{\rm acid} = 335.9 \pm 2.1 \, \rm kcal/mol$ ), pyruvic acid ( $\Delta H_{\rm acid} = 333.5 \pm 2.9 \, \rm kcal/mol$ ), and

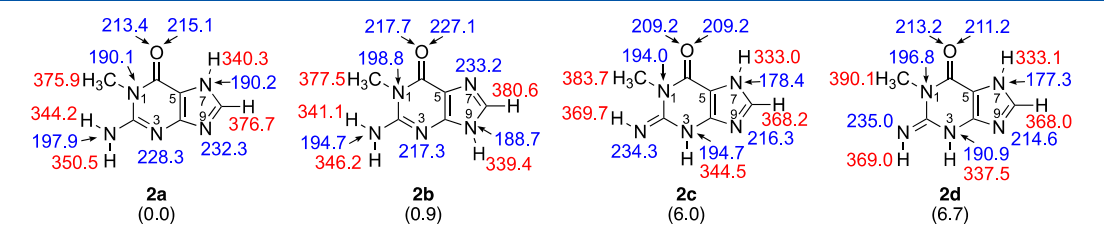


Figure 3. Calculated data for 1-methylguanine. Gas phase acidities are in red; gas phase proton affinities are in blue. Relative stabilities are in parentheses. Calculations were conducted at B3LYP-D3(BJ)/6-311++G(2d,p); reported values are  $\Delta H$  at 298 K, in kcal/mol.

 $\alpha$ , $\alpha$ , $\alpha$ -trifluoro-m-toluic acid ( $\Delta H_{\rm acid} = 332.2 \pm 2.1$  kcal/mol), yielding an acidity of 337  $\pm$  3 kcal/mol.

Experiments: Proton Affinity, 1meG. The PA of 1-methylguanine was measured using six references, which were 4-picoline (PA =  $226.4 \pm 2.0 \text{ kcal/mol}$ ), cytosine (PA =  $227.0 \pm 2.0 \text{ kcal/mol}$ ), piperidine (PA =  $228.0 \pm 2.0 \text{ kcal/mol}$ ), 1-methylimidazole (PA =  $229.3 \pm 2.0 \text{ kcal/mol}$ ), 1-methylpyrrolidine (PA =  $230.8 \pm 2.0 \text{ kcal/mol}$ ), and 1-methylpiperidine (PA =  $232.1 \pm 2.0 \text{ kcal/mol}$ ). The PA was measured to be  $229 \pm 3 \text{ kcal/mol}$ .

**3-Methylthymine (3meT, 3).** *Calculations: Tautomers, Acidity, Proton Affinity, 3meT.* 3-Methylthymine (3meT, 3) is calculated to have one very stable tautomer (Figure 4, 3a). The

**Figure 4.** Calculated data for 3-methylthymine. Gas phase acidities are in red; gas phase proton affinities are in blue. Relative stabilities are in parentheses. Calculations were conducted at B3LYP-D3(BJ)/6-311++G(2d,p); reported values are  $\Delta H$  at 298 K, in kcal/mol.

next most stable tautomer **3b** is 10.7 kcal/mol less stable than **3a**. The most acidic site of **3a** is the N1-H, at 337.5 kcal/mol. The most basic site of tautomer **3a** is on the O4, at 212.6 kcal/mol.

Experiments: Acidity, 3meT. We measured the acidity of 3-methylthymine via bracketing (Table 2). We find that

Table 2. Acidity Bracketing of 3meT (3)

		proton transfer <sup>b</sup>	
reference acid	$\Delta H_{\rm acid}  ({\rm kcal/mol})^a$	ref. acid	conj. base
methyl cyanoacetate	$340.8 \pm 2.1$	-	+
$\alpha, \alpha, \alpha$ -trifluoro- <i>m</i> -cresol	$339.2 \pm 2.1$	_	+
fluoroacetic acid	$339.0 \pm 2.2$	+	+
$\alpha$ , $\alpha$ , $\alpha$ -trifluoro- $p$ -cresol	$337.0 \pm 2.1$	+	_
4,4,4-trifluorobutyric acid	$336.5 \pm 2.9$	+	_
malononitrile	$335.8 \pm 2.1$	+	_

"Reference 23. <sup>b</sup>A "+" indicates the occurrence and "-" indicates the absence of proton transfer.

deprotonated 3meT can deprotonate fluoroacetic acid ( $\Delta H_{\rm acid} = 339.0 \pm 2.2$  kcal/mol) and that fluoroacetate can deprotonate 3meT, allowing us to place the acidity of 3meT at  $339 \pm 3$  kcal/mol.

The acidity of 3meT was also ascertained by the Cooks kinetic method, using 10 reference acids: methoxyacetic acid ( $\Delta H_{\rm acid} = 341.9 \pm 2.1$  kcal/mol), benzoic acid ( $\Delta H_{\rm acid} = 340.1 \pm 2.2$  kcal/mol),  $\alpha,\alpha,\alpha$ -trifluoro-m-cresol ( $\Delta H_{\rm acid} = 339.2 \pm 2.1$  kcal/mol), 3-hydroxybenzoic acid ( $\Delta H_{\rm acid} = 338.6 \pm 2.1$  kcal/mol), anthranilic acid ( $\Delta H_{\rm acid} = 337.3 \pm 2.2$  kcal/mol),  $\alpha,\alpha,\alpha$ -trifluoro-p-cresol ( $\Delta H_{\rm acid} = 337.0 \pm 2.1$  kcal/mol), 3-chloromethyl benzoic acid ( $\Delta H_{\rm acid} = 336.8 \pm 2.1$  kcal/mol), 4,4,4-trifluorobutyric acid ( $\Delta H_{\rm acid} = 336.5 \pm 2.9$  kcal/mol), 4-hydroxybenzoic acid ( $\Delta H_{\rm acid} = 335.9 \pm 2.1$  kcal/mol), and pyruvic acid ( $\Delta H_{\rm acid} = 333.5 \pm 2.9$  kcal/mol). These studies yield a  $\Delta H_{\rm acid}$  of 338  $\pm$  3 kcal/mol.

Experiments: Proton Affinity, 3meT. In bracketing the PA of 3-methylthymine (Table 3), we found that the proton transfer reactions occur in both directions for mesityl oxide (PA = 210.0 kcal/mol), placing the PA of 3-methylthymine at  $210 \pm 3 \text{ kcal/mol}$ .

Table 3. Proton Affinity Bracketing of 3-Methylthymine (3)

		proton transfer <sup>b</sup>	
reference base	PA (kcal/mol) <sup>a</sup>	ref base	conj acid
m-toluidine	$214.1 \pm 2$	+	_
o-toluidine	$212.9 \pm 2$	+	_
2-(trifluoromethyl)pyridine	$212.0 \pm 2$	+	_
2',4'-dimethylacetophenone	$210.9 \pm 2$	+	_
mesityl oxide	$210.0 \pm 2$	+	+
pyrrole	$209.2 \pm 2$	_	+
2,4-pentadione	$208.8 \pm 2$	_	+
3-chloroaniline	$207.5 \pm 2$	_	+

"Reference 23. "A "+" indicates the occurrence and "-" indicates the absence of proton transfer.

The proton affinity of 3-methylthymine was also measured using the Cooks kinetic method. Five reference bases were used, m-toluidine (PA = 214.1  $\pm$  2.0 kcal/mol), o-toluidine (PA = 212.9  $\pm$  2.0 kcal/mol), pyrimidine (PA = 211.7  $\pm$  2.0 kcal/mol), aniline (PA = 210.9  $\pm$  2.0 kcal/mol), and 4-fluoroaniline (PA = 208.3  $\pm$  2.0 kcal/mol), yielding a proton affinity (PA =  $\Delta H$ ) for 3meT of 211  $\pm$  3 kcal/mol.

**3-Methylcytosine (3meC, 4).** Calculations: Tautomers, Acidity, Proton Affinity, 3meC. Three 3meC tautomers are within 10 kcal/mol of the most stable structure (Figure 5).

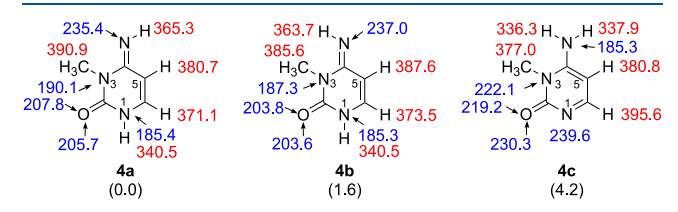


**Figure 5.** Calculated data for 3-methylcytosine. Gas phase acidities are in red; gas phase proton affinities are in blue. Relative stabilities are in parentheses. Calculations were conducted at B3LYP-D3(BJ)/6-311++G(2d,p); reported values are  $\Delta H$  at 298 K, in kcal/mol.

The most stable tautomer (4a) is 1.6 kcal/mol more stable than tautomer 4b. The most acidic site of 4a is predicted to be the N1 proton ( $\Delta H_{\rm acid} = 340.5 \text{ kcal/mol}$ ). The most basic site of tautomer 4a is the exocyclic imine nitrogen (PA = 235.4 kcal/mol). The acidity of 4b is 340.5 kcal/mol, and the PA is 237.0 kcal/mol.

**3-Ethylcytosine (3etC, 5).** Calculations: Tautomers, Acidity, Proton Affinity, 1meA. The four most stable 3-ethylcytosine tautomers are depicted in Figure 6. **5a** is more stable than its imine rotamer **5b** by 2.1 kcal/mol. The most acidic site of **5a** is the N1-H ( $\Delta H_{\rm acid} = 340.3 \text{ kcal/mol}$ ). The most basic site of **5a** is at the exocyclic imine nitrogen, with a PA of 236.4 kcal/mol. The most acidic site of tautomer **5b** is predicted to be the N1-H also ( $\Delta H_{\rm acid} = 340.7 \text{ kcal/mol}$ ); the most basic site of tautomer **5b** is also at N6 (PA = 238.5 kcal/mol).

**1,N**<sup>6</sup>-Ethenoadenine (eA, 6). Calculations: Tautomers, Acidity, Proton Affinity, eA. There are two comparably stable tautomers of  $1,N^6$ -ethenoadenine, the N7H (6a) and the N9H

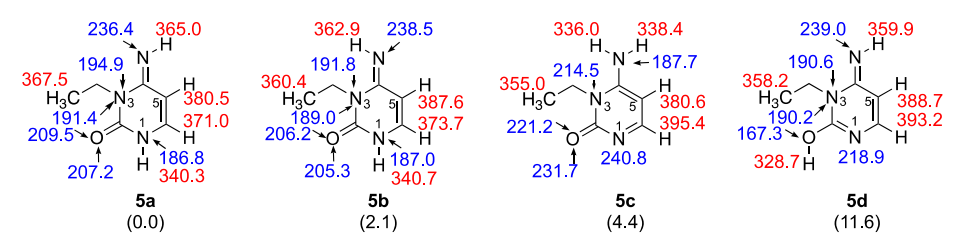


Figure 6. Calculated data for 3-ethylcytosine. Gas phase acidities are in red; gas phase proton affinities are in blue. Relative stabilities are in parentheses. Calculations were conducted at B3LYP-D3(BJ)/6-311++G(2d,p); reported values are  $\Delta H$  at 298 K, in kcal/mol.

(6b, Figure 7). The most acidic site of 6a is the N7 proton, with an acidity of 334.6 kcal/mol. The most basic site is at N9

Figure 7. Calculated data for  $1,N^6$ -ethenoadenine. Gas phase acidities are in red; gas phase proton affinities are in blue. Relative stabilities are in parentheses. Calculations were conducted at B3LYP-D3(BJ)/6-311++G(2d,p); reported values are  $\Delta H$  at 298 K, in kcal/mol.

with a PA of 225.8 kcal/mol. The second most stable tautomer is **6b**, which is just 0.8 kcal/mol higher in energy than **6a**. The proton affinity of **6b** is 235.4 kcal/mol, at the N12 site, and the acidity is calculated to be 333.8 kcal/mol, at the N9-H site.

We previously calculated the thermochemical properties of eA at B3LYP/6-31+G(d) and also measured the acidity ( $\Delta H_{\rm acid} = 332 \pm 3 \text{ kcal/mol}$ ) and PA (PA = 232  $\pm$  4 kcal/mol). Our results are consistent with the prior work.

**1,N**<sup>6</sup>-Ethanoadenine (EA, 7). Calculations: Tautomers, Acidity, Proton Affinity, EA. There are three EA tautomers within 10 kcal/mol of the most stable structure 7a (Figure 8). The N7H tautomer 7a and the N9H tautomer 7b are very close in terms of stability. The most acidic site of 7a is the N7-H, with a calculated  $\Delta H_{\rm acid}$  of 338.5 kcal/mol. The most basic site of 7a is the N12, with a PA of 236.5 kcal/mol. For 7b, the most acidic site has a calculated  $\Delta H_{\rm acid}$  of 338.3 kcal/mol (N9-H), while the most basic site is also the N12 (PA = 245.5 kcal/mol).

**1,**  $N^2$ -Ethenoguanine (1eG, 8). Calculations: Tautomers, Acidity, Proton Affinity, 1eG. 1, $N^2$ -ethenoguanine has three low-lying tautomers that are within 1 kcal/mol of each other (8a, 8b, and 8c, Figure 9). The most acidic site of 8a is predicted to be the N10-H ( $\Delta H_{\rm acid} = 332.3 \text{ kcal/mol}$ ). The most basic site of tautomer 8a is at N9 (PA = 231.4 kcal/mol). For tautomer 8b, which is less stable than 8a by 0.3 kcal/mol,

the acidity is computed to be 329.5 kcal/mol at the N7-H site, while the PA is 226.4 kcal/mol, at the N10 site. For tautomer 8c, the calculated acidity is 330.0 kcal/mol (N10-H) while the PA is 232.4 kcal/mol (N7).

 $N^2$ ,3-Ethenoguanine (3eG, 9). Calculations: Tautomers, Acidity, Proton Affinity, 3eG. 3eG is not believed to be an AlkB substrate but is a commonly studied lesion that is included for comparison purposes.<sup>3</sup> The most stable tautomer of 3eG, 9a, is more stable than 9b by 6.0 kcal/mol (Figure 10). The most acidic site of 9a is the N7-H, with a  $\Delta H_{\rm acid}$  of 327.8 kcal/mol. The most basic site is the N12 site, at 226.2 kcal/mol.

**3,** $N^4$ -Ethenocytosine (eC, 10). Calculations: Tautomers, Acidity, Proton Affinity, eC. Tautomer 10a of 3, $N^4$ -ethenocytosine is more than 10 kcal/mol more stable than the next most stable tautomer 10b (Figure 11). The most acidic site is the N1 proton, at 335.0 kcal/mol. The most basic site is at N7 (227.7 kcal/mol).

Experiments: Acidity, eC. We measured the acidity of eC using acidity bracketing (Table 4). Deprotonated eC is able to deprotonate malononitrile ( $\Delta H_{\rm acid} = 335.8 \pm 2.1 \text{ kcal/mol}$ ); deprotonated malononitrile likewise deprotonates neutral eC. We therefore bracket the  $\Delta H_{\rm acid}$  of  $3,N^4$ -ethenocytosine to be  $336 \pm 4 \text{ kcal/mol}$ .

The acidity of 3, $N^4$ -ethenocytosine was also measured using the Cooks kinetic method. Seven reference acids were used, 4,4,4-trifluorobutyric acid ( $\Delta H_{\rm acid} = 336.5 \pm 2.9 \, \rm kcal/mol)$ , 3-fluorobenzoic acid ( $\Delta H_{\rm acid} = 336.1 \pm 2.1 \, \rm kcal/mol)$ , 4-hydroxybenzoic acid ( $\Delta H_{\rm acid} = 335.9 \pm 2.1 \, \rm kcal/mol)$ , 4-acetylbenzoic acid ( $\Delta H_{\rm acid} = 334.3 \pm 2.1 \, \rm kcal/mol)$ , pyruvic acid ( $\Delta H_{\rm acid} = 333.5 \pm 2.9 \, \rm kcal/mol)$ ),  $\alpha, \alpha, \alpha$ -trifluoro-m-toluic acid ( $\Delta H_{\rm acid} = 332.2 \pm 2.2 \, \rm kcal/mol)$ , and difluoroacetic acid ( $\Delta H_{\rm acid} = 331.0 \pm 2.2 \, \rm kcal/mol)$ , yielding a  $\Delta H_{\rm acid}$  of 335  $\pm$  3 kcal/mol.

Experiments: Proton Affinity, eC. 3-Picoline (PA =  $225.5 \pm 2.0 \text{ kcal/mol}$ ) is able to deprotonate protonated eC; also, eC can deprotonate protonated 3-picoline (Table 5). We therefore bracket the PA of  $3,N^4$ -ethenocytosine to be  $226 \pm 3 \text{ kcal/mol}$ .

We also measured the PA of  $3,N^4$ -ethenocytosine using the Cooks kinetic method. The measurement utilized 10 reference bases: N,N'-dimethylethylenediamine (PA =  $236.4 \pm 2.0 \text{ kcal/}$ 

Figure 8. Calculated data for  $1,N^6$ -ethanoadenine. Gas phase acidities are in red; gas phase proton affinities are in blue. Relative stabilities are in parentheses. Calculations were conducted at B3LYP-D3(BJ)/6-311++G(2d,p); reported values are  $\Delta H$  at 298 K, in kcal/mol.

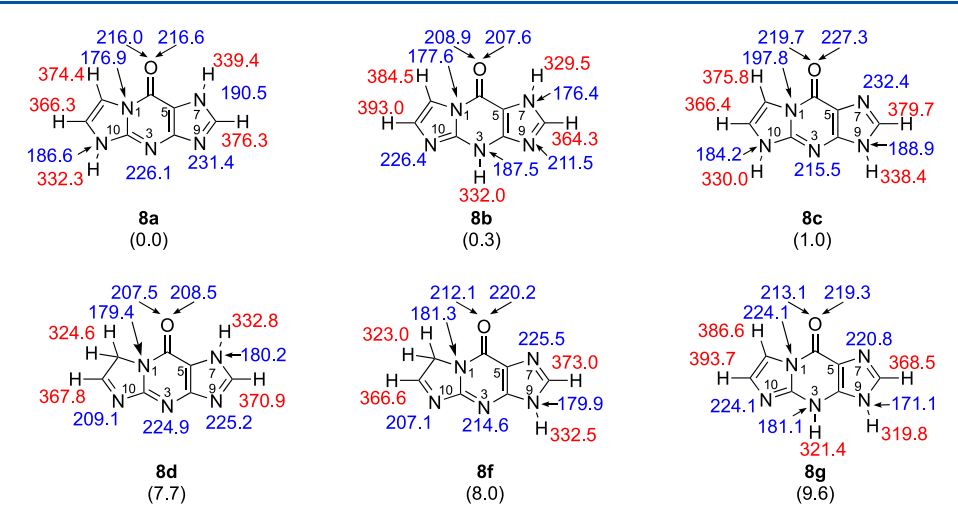


Figure 9. Calculated data for  $1,N^2$ -ethenoguanine. Gas phase acidities are in red; gas phase proton affinities are in blue. Relative stabilities are in parentheses. Calculations were conducted at B3LYP-D3(BJ)/6-311++G(2d,p); reported values are  $\Delta H$  at 298 K, in kcal/mol.

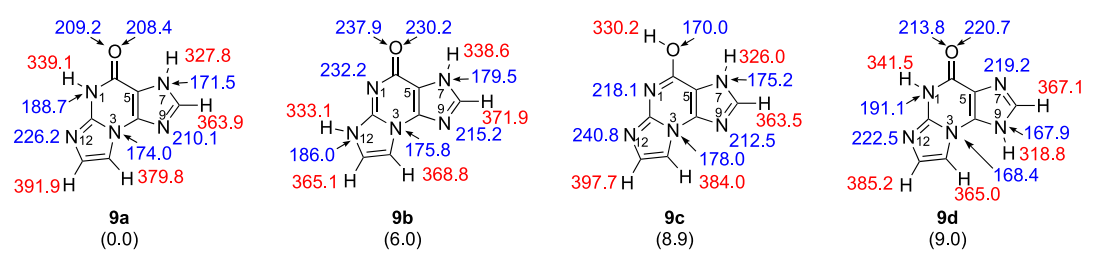
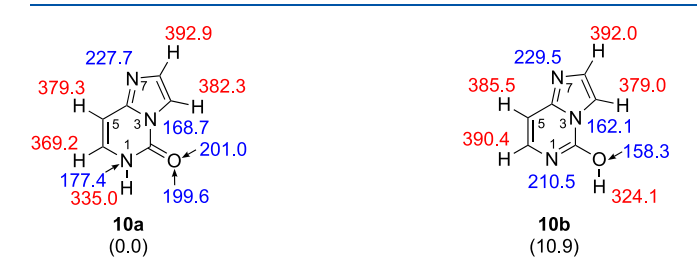


Figure 10. Calculated data for  $N^2$ ,3-ethenoguanine. Gas phase acidities are in red; gas phase proton affinities are in blue. Relative stabilities are in parentheses. Calculations were conducted at B3LYP-D3(BJ)/6-311++G(2d,p); reported values are  $\Delta H$  at 298 K, in kcal/mol.



**Figure 11.** Calculated data for  $3,N^4$ -ethenocytosine. Gas phase acidities are in red; gas phase proton affinities are in blue. Relative stabilities are in parentheses. Calculations were conducted at B3LYP-D3(BJ)/6-311++G(2d,p); reported values are  $\Delta H$  at 298 K, in kcal/mol.

Table 4. Acidity Bracketing of 3,N<sup>4</sup>-Ethenocytosine (10)

		proton transfer <sup>b</sup>	
reference acid	$\Delta H_{\rm acid}  ({\rm kcal/mol})^a$	ref acid	conj base
$\alpha,\alpha,\alpha$ -trifluoro- $m$ -cresol	$339.2 \pm 2.1$	_	+
4,4,4-trifluorobutyric acid	$336.5 \pm 2.9$	_	+
malononitrile	$335.8 \pm 2.1$	+	+
pyruvic acid	$333.5 \pm 2.9$	+	_
difluoroacetic acid	$331.0 \pm 2.2$	+	_

<sup>a</sup>Reference 23. <sup>b</sup>A "+" indicates the occurrence and "–" indicates the absence of proton transfer.

mol), *N*,*N*-dimethylcyclohexylamine (PA = 235.1  $\pm$  2.0 kcal/mol), di-sec-butylamine (PA = 234.4  $\pm$  2.0 kcal/mol), *N*-methylpiperidine (PA = 232.1  $\pm$  2.0 kcal/mol), *N*-methylpyrrolidine (PA = 230.8  $\pm$  2.0 kcal/mol), piperidine (PA = 228.0  $\pm$  2.0 kcal/mol), benzimidazole (PA = 228.0  $\pm$  2.0 kcal/mol)

Table 5. PA Bracketing of  $3N^4$ -Ethenocytosine (10)

		proton transfer <sup>b</sup>	
reference base	PA (kcal/mol) <sup>a</sup>	ref base	conj acid
2,4-lutidine	$230.1 \pm 2.0$	+	_
4-picoline	$226.4 \pm 2.0$	+	_
3-picoline	$225.5 \pm 2.0$	+	+
tert-amylamine	$224.1 \pm 2.0$	_	+
cyclohexylamine	$223.3 \pm 2.0$	_	+

<sup>a</sup>Reference 23. <sup>b</sup>A "+" indicates the occurrence and "–" indicates the absence of proton transfer.

mol), 4-picoline (PA =  $226.4 \pm 2.0 \text{ kcal/mol}$ ), 3-picoline (PA =  $225.5 \pm 2.0 \text{ kcal/mol}$ ), and 3,5-dimethylpyrazole (PA =  $223.1 \pm 2.0 \text{ kcal/mol}$ ), yielding a PA of  $225 \pm 3 \text{ kcal/mol}$ .

#### DISCUSSION

Calculated versus Experimental Values. The calculated and experimental acidity and proton affinity values for all the substrates studied herein are summarized in Table 6. Generally, B3LYP-D3(BJ)/6-311++G(2d,p) appears to provide fairly accurate predictions for the thermochemical values.

**Biological Implications.** *Escherichia coli* AlkA and AlkB are both DNA repair enzymes. AlkA is a glycosylase that processes lesions by excising the damaged base, breaking the *N*-glycosidic bond (Figure 1). AlkB was identified early on, in 1983, but it took nearly 20 years to figure out its precise function; AlkB is a dioxygenase rather than a glycosylase. It effects DNA repair by oxidizing the aberrant groups, followed by restoration of the undamaged DNA base. Therefore, unlike AlkA, which simply excises the damaged base, AlkB directly

Table 6. Calculated (B3LYP-D3(BJ)/6-311++G(2d,p); 298 K) and Experimental Data for Damaged Bases

substrate	calculated value	experimental value <sup>b</sup>
$\Delta H_{ m acid}^{a}$		
1-methyladenine (1meA, 1)	337.4	$334 \pm 3$
1-methylguanine (1meG, 2)	340.3	$(337 \pm 3)$
3-methylthymine (3meT, 3)	337.5	$339 \pm 3 \ (338 \pm 3)$
$1,N^6$ -ethenoadenine (eA, 6)	333.8	$332 \pm 3^{c}$
$3N^4$ -ethenocytosine (eC, 10)	335.0	$336 \pm 4 (335 \pm 3)$
$PA^a$		
1-methyladenine (1meA, 1)	241.6	$239 \pm 3 (244 \pm 3)$
1-methylguanine (1meG, 2)	232.3	$(229 \pm 3)$
3-methylthymine (3meT, 3)	212.6	$210 \pm 3 \ (211 \pm 3)$
$1,N^6$ -ethenoadenine (eA, 6)	235.4	$232 \pm 4^{c}$
$3,N^4$ -ethenocytosine (eC, 10)	227.7	$226 \pm 3 \ (225 \pm 3)$

 $^a\Delta H_{\rm acid}$  and PA values are in kcal/mol.  $^b{\rm The}$  first listed experimental value is bracketed; the Cooks kinetic method value, if available, is in parentheses.  $^c{\rm Reference}$  28.

reverses the base damage at the affected site to yield the repaired, normal base (Figure 1).<sup>3,8,11,12,14,15,29-33</sup>

We are intrigued by why some damaged nucleobases are cleaved by AlkA while others are dealkylated by AlkB. A reasonable hypothesis, and one that others have also proposed, is that damaged bases are processed via excision, unless the *N*-glycosidic bond is too stable—then Nature has to devise an alternative repair pathway. 9,11,34 Our interest is therefore in assessing the *N*-glycosidic bond stability of both AlkA and AlkB substrates; presumably if that bond is labile enough, AlkA will excise it. However, if that bond is too stable, then other enzymes such as AlkB will need to step in to effect repair.

Both enzymes have a broad substrate range, cleaving a wide variety of damaged bases. <sup>1-3</sup> We have found in prior studies that enzymes that accept a large range of substrates often have active sites that are not specific but do provide a hydrophobic environment that can help differentiate among various substrates. <sup>16,17,19,35,36</sup> In such cases, gas phase studies can be useful, as the gas phase is the ultimate nonpolar environment.

In prior work, we examined how AlkA differentiates and cleaves damaged bases with more efficiency than normal bases adenine and guanine.<sup>17</sup> We found that ease of cleavage is related to the intrinsic *N*-glycosidic bond stability; the better a leaving group the damaged nucleobase is, the more easily it is cleaved (Figure 12). Since better leaving groups are generally

Figure 12. AlkA excision.

correlated with acidity, nucleobases that are more acidic at the N9-H (for purines) and N1-H (for pyrimidines) positions should be more easily excised. Furthermore, we hypothesized that a major role of AlkA is to provide a non-nucleobase-specific active site that is hydrophobic, which enhances the differences in acidity between damaged and normal nucleobases, which in turn aids in the discrimination of normal from

damaged bases. In support of this hypothesis, we found that the rate of excision of AlkA substrates tracked with their purine N9-H gas phase acidity: the more acidic a substrate was, the faster the cleavage. We found that these acidity differences were greatest in the gas phase; the aqueous acidities were often almost the same. In a nonpolar environment, the acidities, and therefore the leaving group abilities, of the various damaged bases were differentiable. This provided evidence for the hypothesis that AlkA has a hydrophobic active site that helps differentiate normal from damaged nucleobases.

Because the rate of AlkA excision tracked with gas phase acidity, we further hypothesize that for substrates that are not acidic enough to be cleaved, Nature had to devise a different method for repair.<sup>37</sup> AlkB may be the enzyme that "steps in" when a damaged base is not acidic enough to be easily excised. If this is the case, then one would expect AlkB substrates to be less acidic at the N9-H site than AlkA substrates.

One interesting feature of both AlkA and AlkB is that they process positively charged and neutral nucleobases. For both enzymes, the positively charged substrates are processed more efficiently. 9,14,15,30,38-45 Positively charged substrates arise from certain types of modification; for example, when adenine is alkylated at N1 to form 1meA, the result is a positively charged nucleobase (1aH<sup>+</sup>, Figure 13). Cleavage of that

#### AlkB substrates

#### AlkA substrates

**Figure 13.** Positively charged AlkA and AlkB substrates, and their corresponding calculated acidities. Calculations were conducted at B3LYP-D3(BJ)/6-311++G(2d,p); reported values are  $\Delta H$  at 298 K, in kcal/mol.

positively charged nucleobase results in a neutral nucleobase leaving group; therefore, the relevant acidity to correlate with leaving group ability is the N9-H acidity value for the positively charged substrates. The positively charged substrates for AlkA and AlkB are shown in Figure 13; the acidity values are in blue because they are equivalent to the proton affinity values at those positions for the corresponding neutral substrates. In Figure 13, we see that the three positively charged AlkB substrates, 1meAH<sup>+</sup> ( $\Delta H_{\rm acid}$  = 247.9 kcal/mol), 3meCH<sup>+</sup> ( $\Delta H_{\rm acid}$  = 239.6 kcal/mol), and 3etCH<sup>+</sup> ( $\Delta H_{\rm acid}$  = 240.8 kcal/mol), are all less acidic than the two positively charged AlkA substrates 3-methyladenineH<sup>+</sup> ( $\Delta H_{\rm acid}$  = 235.7 kcal/mol) and 7-methylguanineH<sup>+</sup> ( $\Delta H_{\rm acid}$  = 234.4 kcal/mol). Thus, our results are consistent with the hypothesis that AlkA substrates are the more acidic nucleobases, while AlkB substrates are less

acidic. Because AlkB substrates are less acidic, Nature uses a direct repair mechanism, rather than a cleavage mechanism, to process the lesions.

The neutral substrates and their gas phase acidity values are shown in Figure 14. These follow the same trend; the AlkB

#### AlkB substrates

#### AlkA substrates

**Figure 14.** Neutral AlkA and AlkB substrates, and their corresponding calculated acidities. Calculations were conducted at B3LYP-D3(BJ)/6-311++G(2d,p); reported values are  $\Delta H$  at 298 K, in kcal/mol.

substrates (eC, 3meT, 1eG, 1meG) all have  $\Delta H_{\rm acid}$  values (335.0, 337.5, 338.4, 339.4 kcal/mol, respectively) greater than that of the AlkA substrates (3eG, purine, hypoxanthine; 318.8, 331.1, 333.8 kcal/mol, respectively). A larger  $\Delta H_{\rm acid}$  value would correspond to poorer leaving group ability and, thus, a more stable N-glycosidic bond. Therefore, our results are consistent with the hypothesis that nucleobases with more stable N-glycosidic bonds are less likely to be excised by AlkA and instead are repaired by a different path, which is in this case direct repair by AlkB. Furthermore, these subtle differences in substrate acidity are enhanced in a nonpolar environment and the AlkA and AlkB active sites may provide such an environment to aid in the discrimination among damaged bases.

One caveat is that if AlkA excision were solely based on acidity, one might expect the positively charged AlkB substrates to be cleavable by AlkA. Clearly, there are other factors at play that favor those substrates for AlkB; for example, Kuśmierek and coworkers have found that positively charged substrates (which, unlike AlkA substrates, are charged at the N1/N3 position of purines/pyrimidines (Figure 13)) are stabilized by a well-positioned aspartate group (Asp-135) in the active site. <sup>39</sup> Of course, also, the gas phase is an extreme nonpolar environment that would not be expected to stabilize charge. Still, it is certainly of interest that among the positively charged substrates, the ones that are less acidic in the gas phase are not cleaved by AlkA.

Last, there are two substrates that are processed by both AlkA and AlkB, eA (6) and EA (7, Figure 15). eA is quite acidic ( $\Delta H_{\rm acid}$  = 333.8 kcal/mol), so we would expect it to be excised easily by AlkA. Consistent with our hypothesis, AlkA is believed to predominate in repairing eA, with AlkB acting only in special situations.<sup>14</sup> EA, on the other hand, is not so acidic ( $\Delta H_{\rm acid}$  = 338.3 kcal/mol), so we would expect AlkB to play a larger role in repair. Also consistent with our prediction, AlkA is in fact far less efficient at excising EA than eA.<sup>33</sup>

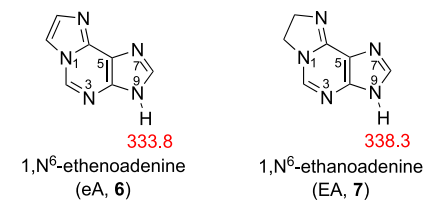


Figure 15. The two lesions processed by both AlkA and AlkB.

Furthermore, EA is found to be extremely toxic when cells are deficient in AlkB, also implying the importance of AlkB in managing this lesion.<sup>33</sup>

# CONCLUSIONS

The relative energies of the possible tautomers, as well as the acidities and proton affinities for a series of AlkB substrates, were calculated and measured in the gas phase, for the first time. Comparison between the gas phase experimental and computational values indicates that B3LYP-D3(BJ)/6-311+ +G(2d,p) is an accurate method and level for calculating these parameters.

The gas phase properties of the substrates were examined in the context of AlkB versus AlkA. Both enzymes repair DNA; however, AlkB reverses damage while AlkA excises the entire damaged nucleobase. We find that more damaged nucleobases that are more acidic at the N9-H position are more likely to be cleaved by AlkA, due to the good leaving group ability of the conjugate base. If a lesion is less acidic at the N9-H position, then it is more likely to be repaired by AlkB, which reverses the damage directly at the affected site. These differences are enhanced in a nonpolar environment, giving support to the hypothesis that AlkA and AlkB both provide a nonspecific, hydrophobic active site that helps differentiate among lesions.

# **■ EXPERIMENTAL SECTION**

All the substrates used herein are commercially available and were used without further purification.

For AlkB substrates (1meA, 3-methylthymine, and 3, $N^4$ -ethenocytosine), acidity and proton affinity were bracketed using a Fourier transform ion cyclotron resonance mass spectrometer (FTMS) with a dual-cell setup, which has been described previously.<sup>35</sup> The magnetic field is 3.3 T, and the baseline pressure in the cells is  $1 \times 10^{-9}$  Torr. AlkB substrates were introduced into the system via a heatable solids probe. The reference acids and bases were introduced via a system of heatable batch inlets or leak valves.<sup>23</sup> Water was pulsed into the cell and ionized by an electron beam to generate either hydroxide (9 eV, 8  $\mu$ A, 0.5 s) or hydronium (20 eV, 6  $\mu$ A, 0.5 s) ions for acidity and proton affinity measurements, respectively.

Reported acidity is the enthalpy of reaction for the transformation shown in eq 1, while proton affinity is the negative of the enthalpy of reaction for the transformation shown in eq 2.

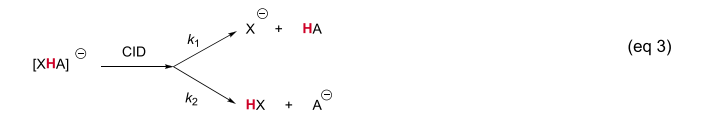
$$HA \rightarrow A^{-} + H^{+} \tag{1}$$

$$B + H^+ \to BH^+ \tag{2}$$

Our protocol for measuring gas phase rate constants has been previously described. Seriefly, taking 3-methylthymine for example, for proton affinity, we generated protonated 3-methylthymine via reaction with hydronium. The protonated 3-methylthymine cations were then selected and transferred from one cubic cell to the other via a 2 mm hole in the middle trapping plate. Transferred ions were cooled with pulsed argon gas that allowed the pressure to rise to  $10^{-5}$  Torr. Reaction with the neutral reference base was then tracked; we also studied the reaction in the "opposite" direction (protonated reference base plus neutral 3-methylthymine). The same methodology is used for acidity, except that deprotonated ions are generated by

reaction with hydroxide. Rapid proton transfer (i.e., measured rate constants near the collisional rate constant) was taken as evidence that the reaction was exothermic and is indicated by a "+" in the tables. Experimental uncertainty (where an endothermic reaction could produce a "+") is estimated to be roughly  $\pm 2$  kcal/mol. The reported values account for this experimental uncertainty as well as the uncertainty in the literature PA and acidity values, which usually range between 2 and 3 kcal/mol. 21,46,47 Experiments were conducted at ambient temperature. Since the amount of the neutral substrate is in excess relative to the reactant ions, these reactions are pseudo first order. Using the ion gauges to ascertain the pressure of the neutral reactants is not always accurate; we instead "back out" the pressure of the neutral substrate from fast control reactions (described previously). 35,48,49 We also note that for one substrate, 1meA, the neutral pressure was such that the PA experiments required a longer equilibration time after generating the protonated 1meAH+ ion; details are in the Supporting Information.

We also measured gas-phase acidity and proton affinity using the Cooks kinetic method.  $^{23-27}$  Briefly, for acidity, a proton-bound dimer was generated between a reference acid HA with a known acidity and the nucleobase HX (eq 3).



The proton-bound dimer was isolated, and then collision-induced dissociation (CID) was used to dissociate the complex into monomeric anions, either deprotonated nucleobase (via  $k_1$ ) or deprotonated reference acid (via  $k_2$ ). We can relate the rate constants ( $k_1$  and  $k_2$ ) to the acidity ( $\Delta H_{\rm acid}$ ) of the unknown nucleobases, as shown in eq 4:

$$\ln\left(\frac{k_1}{k_2}\right) \approx \ln\left(\frac{[X^-]}{[A^-]}\right) = \frac{1}{RT_{\text{eff}}} (\Delta H_{\text{acid}}(HA) - \Delta H_{\text{acid}}(HX)) \tag{4}$$

where R is the gas constant and  $T_{\rm eff}$  is the effective temperature (in kelvin) of the activated complex. Given the assumptions that there is no reverse activation energy barrier in the dissociation process and that the dissociation transition structure is late, the relative acidity of the two compounds is represented by the ratio of the intensities of the two deprotonated products in eq. 4. These assumptions are generally true for proton-bound systems. The acidities for a series of reference acids and the natural logarithm of the relative intensity ratios are plotted linearly to generate a slope of  $(1/RT_{\rm eff})$  and a y-intercept of  $(-\Delta H_{\rm acid}(HX)/RT_{\rm eff})$ .

The proton-bound dimers were prepared in methanol, at a concentration of  $5\times 10^{-5}$  M. The dimers were vaporized via electrospray ionization (ESI), with a needle voltage of 2–4.5 kV. The sheath gas flow rate was  $25~\mu \rm L/min$ . The proton-bound complex ions are activated for 30 ms before isolation and then dissociated by CID, to yield the dissociated monomeric ions. The ratio of the dissociated anions was used to determine the experimental acidity. A total of 40 scans were averaged for each spectrum. The same method was used for proton affinity measurements. As with the bracketing experiments, the reported values account for experimental and literature PA and acidity value uncertainty.  $^{21,46,47}$  We also run three trials of each experiment, to capture precision.

Calculations were conducted at B3LYP-D3(BJ)/6-311++G- $(2d,p)^{52-55}$  using Gaussian16; <sup>56</sup> the geometries were fully optimized, and frequencies were calculated. All the values reported are enthalpies at 298 K.

#### ASSOCIATED CONTENT

# **Data Availability Statement**

All underlying data are available in the article itself and its Supporting Information.

## Supporting Information

The Supporting Information is available free of charge at https://pubs.acs.org/doi/10.1021/acs.joc.3c01335.

Bracketing method; Cooks kinetic method; calculated structures (1-methyladenine, 1meA); calculated structures (1-methyladenineH+, 1meAH+); calculated structures (3-methylcytosine, 3meC); calculated structures (3-methylcytosineH<sup>+</sup>, 3meCH<sup>+</sup>); calculated structures (3-ethylcytosine, 3etC); calculated structures (3-ethylcytosineH<sup>+</sup>, 3etCH<sup>+</sup>); calculated structures (3-methylthymine, 3meT); calculated structures (1-methylguanine, 1meG); calculated structures  $(1,N^{\circ}$ -ethenoadenine, eA); calculated structures  $(3,N^4$ -ethenocytosine, eC); calculated structures (1,No-ethanoadenine, EA); calculated structures  $(1,N^2$ -ethenoguanine, 1N2eG); calculated structures ( $N^2$ ,3-ethenoguanine, N23eG); detailed coordinate information (1-methyladenineH+, 1meAH+), B3LYP-D3(BJ)/6-311++G(2d,p); detailed coordinate information (1-methyladenine, 1meA), B3LYP-D3(BJ)/6-311++G(2d,p); detailed coordinate information (3-methylcytosineH<sup>+</sup>, 3meCH<sup>+</sup>), B3LYP-D3(BJ)/ 6-311++G(2d,p); detailed coordinate information (3methylcytosine, 3meC), B3LYP-D3(BJ)/6-311++G-(2d,p); detailed coordinate information (3-ethylcytosi $neH^+$ ,  $3etCH^+$ ), B3LYP-D3(BJ)/6-311++G(2d,p); detailed coordinate information (3-ethylcytosine, 3etC), B3LYP-D3(BJ)/6-311++G(2d,p); detailed coordinate information (3-methylthymine, 3meT), B3LYP-D3(BJ)/6-311++G(2d,p); detailed coordinate information (1-methylguanine, 1meG), B3LYP-D3(BJ)/6-311+ +G(2d,p); detailed coordinate info  $(1,N^6)$ -ethenoadenine, eA) B3LYP-D3(BJ)/6-311++G(2d,p) method; detailed coordinate information  $(1,N^2$ -ethenoguanine, 1N2eG), B3LYP-D3(BJ)/6-311++G(2d,p); detailed coordinate info  $(1,N^6$ -ethanoadenine, EA) B3LYP-D3(BJ)/6-311++G(2d,p) method; detailed coordinate information  $(3,N^4$ -ethenocytosine, eC), B3LYP-D3(BJ)/ 6-311++G(2d,p); detailed coordinate information  $(N^2,3$ -ethenoguanine, N2,3eG) B3LYP-D3(BJ)/6-311+ +G(2d,p) method; detailed coordinate information  $(3\text{meAH}^+)$ , B3LYP-D3(BJ)/6-311++G(2d,p); detailed coordinate information (7meGH+), B3LYP-D3(BJ)/6-311++G(2d,p); detailed coordinate information (adenine, a), B3LYP-D3(BJ)/6-311++G(2d,p); detailed coordinate information (purine, p), B3LYP-D3(BJ)/6-311++G(2d,p) (PDF)

# AUTHOR INFORMATION

## **Corresponding Author**

Jeehiun K. Lee – Department of Chemistry and Chemical Biology, Rutgers, The State University of New Jersey, New Brunswick, New Jersey 08901, United States; ⊚ orcid.org/ 0000-0002-1665-1604; Email: jee.lee@rutgers.edu

# **Authors**

Lanxin Zhang – Department of Chemistry and Chemical Biology, Rutgers, The State University of New Jersey, New Brunswick, New Jersey 08901, United States

Xiao Ding – Department of Chemistry and Chemical Biology, Rutgers, The State University of New Jersey, New Brunswick, New Jersey 08901, United States Catherine R. Kratka — Department of Chemistry and Chemical Biology, Rutgers, The State University of New Jersey, New Brunswick, New Jersey 08901, United States Alec Levine — Department of Chemistry and Chemical Biology, Rutgers, The State University of New Jersey, New Brunswick, New Jersey 08901, United States

Complete contact information is available at: https://pubs.acs.org/10.1021/acs.joc.3c01335

#### Notes

The authors declare no competing financial interest.

#### ACKNOWLEDGMENTS

We thank the NSF for financial support. For the TOC graphic, AlkA and AlkB images courtesy of RCSB PDB (PDB ID 1MPG, https://doi.org/10.2210/pdb1mpg/pdb and PDB ID 4RFR, https://doi.org/10.2210/pdb4rfr/pdb).

# REFERENCES

- (1) Stivers, J. T.; Jiang, Y. L. A Mechanistic Perspective on the Chemistry of DNA Repair Glycosylases. *Chem. Rev.* **2003**, *103*, 2729–2760.
- (2) Berti, P. J.; McCann, J. A. B. Toward a Detailed Understanding of Base Excision Repair Enzymes: Transition State and Mechanistic Analyses of N-Glycoside Hydrolysis and N-Glycoside Transfer. *Chem. Rev.* 2006, 106, 506–555.
- (3) Fedeles, B. I.; Singh, V.; Delaney, J. C.; Li, D.; Essigmann, J. M. The AlkB Family of Fe(II)/ $\alpha$ -Ketoglutarate-dependent Dioxygenases: Repairing Nucleic Acid Alkylation Damage and Beyond. *J. Biol. Chem.* **2015**, 290, 20734–20742.
- (4) Felske, L. R.; Lenz, S. A. P.; Wetmore, S. D. Quantum Chemical Studies of the Structure and Stability of *N*-Methylated DNA Nucleobase Dimers: Insights into the Mutagenic Base Pairing of Damaged DNA. *J. Phys. Chem. A* **2018**, *122*, 410–419.
- (5) Lenz, S. A. P.; Li, D.; Wetmore, S. D. Insights into the Direct Oxidative Repair of Etheno Lesions: MD and QM/MM Study on the Substrate Scope of ALKBH2 and AlkB. *DNA Repair* **2020**, *96*, No. 102944.
- (6) Samson, L.; Cairns, J. A New Pathway for DNA Repair in Escherichia coli. Nature 1977, 267, 281–283.
- (7) Aravind, L.; Koonin, E. V. The DNA-repair Protein AlkB, EGL-9, and Leprecan Define New Families of 2-Oxoglutarate- and Iron-Dependent Dioxygenases. *Genome Biol.* **2001**, *2*, RESEARCH0007.
- (8) Sedgwick, B. Repairing DNA-Methylation Damage. *Nat. Rev. Mol. Cell Biol.* **2004**, *5*, 148–157.
- (9) Sedgwick, B.; Bates, P. A.; Paik, J.; Jacobs, S. C.; Lindahl, T. Repair of Alkylated DNA: Recent Advances. *DNA Repair* **2007**, *6*, 429–442.
- (10) Shen, L.; Song, C.-X.; He, C.; Zhang, Y. Mechanism and Function of Oxidative Reversal of DNA and RNA Methylation. *Annu. Rev. Biochem.* **2014**, *83*, 585–614.
- (11) Trewick, S. C.; Henshaw, T. F.; Hausinger, R. P.; Lindahl, T.; Sedgwick, B. Oxidative Demethylation by *Escherichia coli* AlkB Directly Reverts DNA Base Damage. *Nature* **2002**, *419*, 174–178.
- (12) Falnes, P. Ø.; Johansen, R. F.; Seeberg, E. AlkB-Mediated Oxidative Demethylation Reverses DNA Damage in *Escherichia coli*. *Nature* **2002**, *419*, 178–182.
- (13) Chen, B. J.; Carroll, P.; Samson, L. The *Escherichia coli* AlkB Protein Protects Human Cells Against Alkylation-Induced Toxicity. *J. Bacteriol.* **1994**, *176*, 6255–6261.
- (14) Delaney, J. C.; Smeester, L.; Wong, C.; Frick, L. E.; Taghizadeh, K.; Wishnok, J. S.; Drennan, C. L.; Samson, L. D.; Essigmann, J. M. AlkB Reverses Etheno DNA Lesions Caused by Lipid Oxidation *in vitro* and *in vivo*. *Nat. Struct. Mol. Biol.* **2005**, 12, 855–860.
- (15) Maciejewska, A. M.; Ruszel, K. P.; Nieminuszczy, J.; Lewicka, J.; Sokołowska, B.; Grzesiuk, E.; Kuśmierek, J. T. Chloroacetaldehyde-

- induced Mutagenesis in *Escherichia coli*: The Role of AlkB Protein in Repair of  $3,N^4$ -Ethenocytosine and  $3,N^4$ - $\alpha$ -Hydroxyethanocytosine. *Mutat. Res.* **2010**, *684*, 24–34.
- (16) Michelson, A. Z.; Rozenberg, A.; Tian, Y.; Sun, X.; Davis, J.; Francis, A. W.; O'Shea, V. L.; Halasyam, M.; Manlove, A. H.; David, S. S.; Lee, J. K. Gas-Phase Studies of Substrates for the DNA Mismatch Repair Enzyme MutY. J. Am. Chem. Soc. 2012, 134, 19839–19850.
- (17) Michelson, A. Z.; Chen, M.; Wang, K.; Lee, J. K. Gas-Phase Studies of Purine 3-Methyladenine DNA Glycosylase II (AlkA) Substrates. *J. Am. Chem. Soc.* **2012**, *134*, 9622–9633.
- (18) Kiruba, G. S. M.; Xu, J.; Zelikson, V.; Lee, J. K. Gas-Phase Studies of Formamidopyrimidine Glycosylase (Fpg) Substrates. *Chem. Eur. J.* **2016**, *22*, 3881–3890.
- (19) Zhang, L.; Hinz, D. J.; Kiruba, G. S. M.; Ding, X.; Lee, J. K. Gas-Phase Experimental and Computational Studies of Human Hypoxanthine-Guanine Phosphoribosyltransferase Substrates: Intrinsic Properties and Biological Implications. *J. Phys. Org. Chem.* **2022**, e4343—e4356.
- (20) Krajewski, A. E.; Lee, J. K. Gas-Phase Experimental and Computational Studies of 5-Halouracils: Intrinsic Properties and Biological Implications. *J. Org. Chem.* **2021**, *86*, 6361–6370.
- (21) Sharma, S.; Lee, J. K. Gas-Phase Acidity Studies of Multiple Sites of Adenine and Adenine Derivatives. *J. Org. Chem.* **2004**, *69*, 7018–7025.
- (22) While the acidity at the time was reported as 331 kcal/mol, a revisit of the bracketing data implies an acidity closer to that of pyruvic acid ( $\Delta H_{\rm acid} = 333.5~{\rm kcal/mol}$ ) since the proton transfer reactions are observed in both directions.
- (23) Linstrom, P. J.; Mallard, W. G. "NIST Chemistry WebBook, NIST Standard Reference Database Number 69." NIST Chemistry WebBook, NIST Standard Reference Database Number 69, National Institute of Standards and Technology, Gaithersburg MD, 20899, http://webbook.nist.gov.
- (24) Cooks, R. G.; Kruger, T. L. Intrinsic Basicity Determination Using Metastable Ions. J. Am. Chem. Soc. 1977, 99, 1279–1281.
- (25) McLuckey, S. A.; Cameron, D.; Cooks, R. G. Proton Affinities from Dissociations of Proton-Bound Dimers. *J. Am. Chem. Soc.* **1981**, 103, 1313–1317.
- (26) McLuckey, S. A.; Cooks, R. G.; Fulford, J. E. Gas-Phase Thermochemical Information from Triple Quadrupole Mass Spectrometers: Relative Proton Affinities of Amines. *Int. J. Mass Spectrom. Ion Phys.* **1983**, *52*, 165–174.
- (27) Green-Church, K. B.; Limbach, P. A. Mononucleotide Gas-Phase Proton Affinities as Determined by the Kinetic Method. *J. Am. Soc. Mass Spectrom.* **2000**, *11*, 24–32.
- (28) Liu, M.; Xu, M.; Lee, J. K. The Acidity and Proton Affinity of the Damaged Base 1,N<sup>6</sup>-Ethenoadenine in the Gas Phase versus in Solution: Intrinsic Reactivity and Biological Implications. *J. Org. Chem.* **2008**, 73, 5907–5914.
- (29) Kataoka, H.; Yamamoto, Y.; Sekiguchi, M. A New Gene (AlkB) of Escherichia coli that Controls Sensitivity to Methyl Methane Sulfonate. *Nature* **1983**, *153*, 1301–1307.
- (30) Delaney, J. C.; Essigmann, J. M. Mutagenesis, Genotoxicity, and Repair of 1-Methyladenine, 3-Alkylcyotsines, 1-Methylguanine and 3-Methylthymine in *alkB Escherichia coli. Proc. Natl. Acad. Sci. U. S. A.* **2004**, *101*, 14051–14056.
- (31) Roy, T. W.; Bhagwat, A. S. Kinetic Studies of *Escherichia coli* AlkB using a New Fluorescence-Based Assay for DNA Demethylation. *Nucleic Acids Res.* **2007**, *35*, No. e147.
- (32) Zdżalik, D.; Domańska, A.; Prorok, P.; Kosicki, K.; van den Born, E.; Falnes, P. Ø.; Rizzo, C. J.; Guengerich, F. P.; Tudek, B. Differential Repair of Etheno-DNA Adducts by Bacterial and Human AlkB Proteins. *DNA Repair* **2015**, *30*, 1–10.
- (33) Li, D.; Delaney, J. C.; Page, C. M.; Yang, X.; Chen, A. S.; Wong, C.; Drennan, C. L.; Essigmann, J. M. Exocyclic Carbons Adjacent to the *N*<sup>6</sup> of Adenine are Targets for Oxidation by the *Escherichia coli* Adaptive Response Protein AlkB. *J. Am. Chem. Soc.* **2012**, *134*, 8896–8901.

- (34) Berdal, K. G.; Johansen, R. F.; Seeberg, E. Release of Normal Bases from Intact DNA by a Native DNA Repair Enzyme. *EMBO J.* **1998**, *17*, 363–367.
- (35) Kurinovich, M. A.; Lee, J. K. The Acidity of Uracil from the Gas Phase to Solution: The Coalescence of the N1 and N3 Sites and Implications for Biological Glycosylation. *J. Am. Chem. Soc.* **2000**, *122*, 6258–6262.
- (36) Lotsof, E. R.; Krajewski, A. E.; Anderson-Steele, B.; Rogers, J.; Zhang, L.; Yeo, J.; Conlon, S. G.; Manlove, A. H.; Lee, J. K.; David, S. S. NEIL1 Recoding due to RNA Editing Impacts Lesion-Specific Recognition and Excision. *J. Am. Chem. Soc.* **2022**, *144*, 14578–14589.
- (37) It is of course possible that Nature developed AlkB first and AlkA second.
- (38) O'Brien, P. J.; Ellenberger, T. The *Escherichia coli* 3-Methyladenine DNA Glycosylase AlkA Has a Remarkably Versatile Active Site. *J. Biol. Chem.* **2004**, *279*, 26876–26884.
- (39) Maciejewska, A. M.; Poznański, J.; Kaczmarska, Z.; Krowisz, B.; Nieminuszczy, J.; Polkowska-Nowakowska, A.; Grzesiuk, E.; Kuśmierek, J. T. AlkB Dioxygenase Preferentially Repairs Protonated Substrates. J. Biol. Chem. 2013, 288, 432.
- (40) Koivisto, P.; Robins, P.; Lindahl, T.; Sedgwick, B. Demethylation of 3-Methylthymine in DNA by Bacterial and Human DNA Dioxygenase. *J. Biol. Chem.* **2004**, *279*, 40470–40474.
- (41) Falnes, P. O. Repair of 3-Methylthymine and 1-Methylguanine Lesions by Bacterial and Human AlkB Proteins. *Nucleic Acids Res.* **2004**, 32, 6260–6267.
- (42) Yi, C.; Jia, G.; Hou, G.; Dai, Q.; Zhang, W.; Zheng, G.; Jian, X.; Yang, C. G.; Cui, Q.; He, C. Iron-Catalysed Oxidation Intermediates Captured in a DNA Repair Dioxygenase. *Nature* **2010**, *468*, 330–333.
- (43) Koivisto, P.; Duncan, T.; Lindahl, T.; Sedgwick, B. Minimal Methylated Substrate and Extended Substrate Range of *Escherichia coli* AlkB Protein, a 1-Methyladenine-DNA Dioxygenase. *J. Biol. Chem.* **2003**, 278, 44348–44354.
- (44) Yu, B.; Edstrom, W. C.; Benach, J.; Hamuro, Y.; Weber, P. C.; Gibney, B. R.; Hunt, J. F. Crystal Structures of Catalytic Complexes of the Oxidative DNA/RNA Repair Enzyme AlkB. *Nature* **2006**, 439, 879–884.
- (45) Duncan, T.; Trewick, S. C.; Koivisto, P.; Bates, P. A.; Lindahl, T.; Sedgwick, B. Reversal of DNA Alkylation Damage by Two Human Dioxygenases. *Proc. Natl. Acad. Sci.* **2002**, *99*, 16660–16665.
- (46) Gronert, S.; Feng, W. Y.; Chew, F.; Wu, W. The Gas Phase Acid/Base Properties of 1,3,-Dimethyluracil, 1-Methyl-2-pyridone, and 1-Methyl-4-pyridone: Relevance to the Mechanism of Orotidine 5'-Monophosphate Decarboxylase. *Int. J. Mass Spectrom.* **2000**, *196*, 251–258.
- (47) Sun, X.; Lee, J. K. Acidity and Proton Affinity of Hypoxanthine in the Gas Phase versus in Solution: Intrinsic Reactivity and Biological Implications. *J. Org. Chem.* **2007**, *72*, 6548–6555.
- (48) Chesnavich, W. J.; Su, T.; Bowers, M. T. Collisions in a Noncentral Field: A Variational and Trajectory Investigation of Ion-Dipole Capture. *J. Chem. Phys.* **1980**, 72, 2641–2655.
- (49) Su, T.; Chesnavich, W. J. Parametrization of the Ion-Polar Molecule Collision Rate Constant by Trajectory Calculations. *J. Chem. Phys.* **1982**, *76*, 5183–5185.
- (50) Drahos, L.; Vékey, K. How Closely Related Are the Effective and the Real Temperature. *J. Mass. Spectrom.* **1999**, 34, 79-84.
- (51) Ervin, K. M. Experimental Techniques in Gas-Phase Ion Thermochemistry. *Chem. Rev.* **2001**, *101*, 391–444.
- (52) Lee, C.; Yang, W.; Parr, R. G. Development of the Colle-Salvetti Correlation-Energy Formula into a Functional of the Electron Density. *Phys. Rev. B* **1988**, *37*, 785–789.
- (53) Kohn, W.; Becke, A. D.; Parr, R. G. Density-Functional Theory of Electronic Structure. *J. Phys. Chem.* **1996**, *100*, 12974–12980.
- (54) Becke, A. D. Density-Functional Thermochemistry. III. The Role of Exact Exchange. *J. Chem. Phys.* **1993**, 98, 5648–5652.
- (55) Grimme, S.; Ehrlich, S.; Goerigk, L. Effect of the Damping Function in Dispersion Corrected Density Functional Theory. *J. Comput. Chem.* **2011**, 32, 1456–1465.

(56) Gaussian 16, Rev. B.; Frisch, M. J.; Trucks, G. W.; Schlegel, H. B.; Scuseria, G. E.; Robb, M. A.; Cheeseman, J. R.; Scalmani, G.; Barone, V.; Petersson, G. A.; Nakatsuji, H.; Li, X.; Caricato, M.; Marenich, A. V.; Bloino, J.; Janesko, B. G.; Gomperts, R.; Mennucci, B.; Hratchian, H. P.; Ortiz, J. V.; Izmaylov, A. F.; Sonnenberg, J. L.; Williams-Young, D.; Ding, F.; Lipparini, F.; Egidi, F.; Goings, J.; Peng, B.; Petrone, A.; Henderson, T.; Ranasinghe, D.; Zakrzewski, V. G.; Gao, J.; Rega, N.; Zheng, G.; Liang, W.; Hada, M.; Ehara, M.; Toyota, K.; Fukuda, R.; Hasegawa, J.; Ishida, M.; Nakajima, T.; Honda, Y.; Kitao, O.; Nakai, H.; Vreven, T.; Throssell, K.; MontgomeryE, J. A., Jr.; Peralta, J. E.; Ogliaro, F.; Bearpark, M. J.; Heyd, J. J.; Brothers, E. N.; Kudin, K. N.; Staroverov, V. N.; Keith, T. A.; Kobayashi, R.; Normand, J.; Raghavachari, K.; Rendell, A. P.; Burant, J. C.; Iyengar, S. S.; Tomasi, J.; Cossi, M.; Millam, J. M.; Klene, M.; Adamo, C.; Cammi, R.; Ochterski, J. W.; Martin, R. L.; Morokuma, K.; Farkas, O.; Foresman, J. B.; Fox, D. J.", Gaussian, Inc., Wallingford CT, 2016.